RESEARCH ARTICLE

Enhancing electrical outputs of the fuel cells with *Geobacter sulferreducens* by overexpressing nanowire proteins

Zhigao Wang[1] | Yidan Hu[1,2] | Yiran Dong[1,2,3,4,5] | Liang Shi[1,3,4,5] |
Yongguang Jiang[1,2]

[1]Department of Biological Sciences and Technology, School of Environmental Studies, China University of Geosciences, Wuhan, Hubei, China

[2]Hubei Key Laboratory of Wetland Evolution and Eco-Restoration, Wuhan, Hubei, China

[3]State Key Laboratory of Biogeology and Environmental Geology, China University of Geosciences, Wuhan, Hubei, China

[4]Hubei Key Laboratory of Yangtze Catchment Environmental Aquatic Science, China University of Geosciences, Wuhan, Hubei, China

[5]State Environmental Protection Key Laboratory of Source Apportionment and Control of Aquatic Pollution, Ministry of Ecology and Environment, China University of Geosciences, Wuhan, Hubei, China

Correspondence
Yongguang Jiang and Liang Shi, No. 388 Lumo Road, Hongshan District, Wuhan, Hubei 430074, China.
Email: jiangyg@cug.edu.cn and liang.shi@cug.edu.cn

Funding information
National Key Research and Development Program of China, Grant/Award Number: 2018YFA0901303; National Natural Science Foundation of China, Grant/Award Number: 41772363 and 91851211; Fundamental Research Funds for the Central Universities

Abstract

Protein nanowires are critical electroactive components for electron transfer of *Geobacter sulfurreducens* biofilm. To determine the applicability of the nanowire proteins in improving bioelectricity production, their genes including *pilA*, *omcZ*, *omcS* and *omcT* were overexpressed in *G. sulfurreducens*. The voltage outputs of the constructed strains were higher than that of the control strain with the empty vector (0.470–0.578 vs. 0.355 V) in microbial fuel cells (MFCs). As a result, the power density of the constructed strains (i.e. 1.39–1.58 W m^{-2}) also increased by 2.62- to 2.97-fold as compared to that of the control strain. Overexpression of nanowire proteins also improved biofilm formation on electrodes with increased protein amount and thickness of biofilms. The normalized power outputs of the constructed strains were 0.18–0.20 W g^{-1} that increased by 74% to 93% from that of the control strain. Bioelectrochemical analyses further revealed that the biofilms and MFCs with the constructed strains had stronger electroactivity and smaller internal resistance, respectively. Collectively, these results demonstrate for the first time that overexpression of nanowire proteins increases the biomass and electroactivity of anode-attached microbial biofilms. Moreover, this study provides a new way for enhancing the electrical outputs of MFCs.

INTRODUCTION

Microbial extracellular electron transfer (EET) is an important metabolic process, in which microorganisms exchange electrons with various extracellular acceptors such as metal oxides, organic compounds and electrodes (Jiang et al., 2019; Logan et al., 2019; Shi et al., 2016). The microorganisms with the capability to exchange electrons with electrodes are called as electroactive microbes that have shown great promise

as biocatalysts in bioelectrochemical systems (BESs) for various biotechnological applications (Logan et al., 2019; Shi et al., 2019). One of extensively studied BESs is microbial fuel cells (MFCs) in which electro-active microbes convert chemical energy to electrical energy through transferring electrons, generated by the oxidation of organic substrates, to electrodes via EET (Santoro et al., 2017; Verma et al., 2021). Therefore, MFC is an attractive bioelectrochemical technology for coupling wastewater treatment and energy recovery from organic matter (Santoro et al., 2017, Verma et al., 2021). However, the applications of MFCs have practically stagnated due to low output of power density (Mateo et al., 2018).

Electroactivity of microbes is a primary bottleneck for improving electricity production of MFCs (Zhao et al., 2020). *Geobacter* spp. are promising for bioelec-trochemical applications because of a strong capacity for EET (Reguera & Kashefi, 2019). For example, *G. sulfurreducens* generates the highest current density of wild-type microbes available in pure culture (Nevin et al., 2008; Rotaru et al., 2015; Yi et al., 2009). The electrical output of MFCs is significantly impacted by the thickness and conductivity of *G. sulfurreducens* biofilm grown on the surfaces of electrodes (Hu et al., 2021; Malvankar et al., 2012; Reguera et al., 2006; Steidl et al., 2016). Generally, thick biofilms with high conductivity are expected to generate high current density. On the other hand, biofilm conductivity is a decisive variable for biofilm thickness (Steidl et al., 2016). The conductivity of *G. sulfurreducens* biofilm is conferred by membrane-bound and matrix-associated electroactive *c*-type cytochromes and protein nanowires (Jiménez Otero et al., 2021; Liu et al., 2021; Malvankar et al., 2012; Richter et al., 2009, 2012; Yalcin et al., 2020).

Geobacter sulfurreducens nanowires are conductive filaments with the base anchored in cell membrane and the distal end extending through the biofilm (Liu et al., 2021; Wang et al., 2019; Yalcin et al., 2020). The nanowires could transfer electrons from bacterial membrane to extracellular electrodes by direct contact (Liu et al., 2020; Reguera et al., 2005; Wang et al., 2019; Yalcin et al., 2020). Previous study revealed that EET across membrane and through the biofilm are two limiting steps for catalytic current generation (Strycharz et al., 2011). Therefore, protein nanowires are ideal targets for genetic engineering of *G. sulfurreducens* to improve electrical output of MFCs (Dantas et al., 2015; Leang et al., 2013).

Geobacter sulfurreducens has been proposed to generate two types of nanowires, namely, conductive pili (e-pili) comprising PilA protein (Liu et al., 2021) and *c*-type cytochrome filaments comprising OmcZ or OmcS proteins (Wang et al., 2019; Yalcin et al., 2020). E-pili and OmcZ are required for thick electroactive biofilm and optimal current production of *G. sulfurreducens* (Nevin et al., 2009; Reguera et al., 2005, 2006; Steidl et al., 2016; Vargas et al., 2013). However,

deletion of OmcS and its homologue OmcT did not impair the current production of *G. sulfurreducens* (Nevin et al., 2009). Previous study suggested that the reciprocal relationship between expressions of *omcS* and *omcZ* genes may render the role of OmcS in current production underappreciated (Wang et al., 2019, Yalcin et al., 2020). In addition, OmcZ is highly concentrated at the biofilm–electrode interface and may serve as an electrochemical gate facilitating electron transfer from biofilm to the electrode (Inoue et al., 2011). The EET efficiency of *G. sulfurreducens* could not be improved by replacing the endogenous e-pili with the more conductive one from *G. metallireducens* (Tan et al., 2017). On the contrary, the *G. sulfurreducens* variants with greater abundance of e-pili and *c*-type cytochromes have stronger capacity for current production in MFCs than the wild type (Hernández-Eligio et al., 2022; Leang et al., 2013; Yi et al., 2009). These findings indicated that the abundance of nanowires may be critical for enhancing EET efficiency of *G. sulfurreducens*. To determine whether nanowire proteins are applicable for further improving the electrical output of MFCs, the genes encoding PilA, OmcZ, OmcS and OmcT proteins were overexpressed in *G. sulfurreducens* via a high-copy-number vector in this study. The results show for the first time the enhanced electricity production of *G. sulfurreducens* MFCs via overexpression of bacterial nanowire proteins.

EXPERIMENTAL PROCEDURE

Bacterial strains and growth conditions

Wild-type *G. sulfurreducens* PCA (ATCC 51573) was obtained from the American Type Culture Collection. *G. sulfurreducens* strains were routinely grown anaerobically in NBFA medium (Coppi et al., 2001). The gas phase was 80% N_2 and 20% CO_2. All the procedures referring to *Geobacter* cells were performed in an anaerobic chamber (Coy Laboratory Products) that was filled with 5% H_2, 20% CO_2 and 75% N_2. *Escherichia coli* DH5α was cultured in Luria-Bertani (LB) medium and used for gene cloning experiments. Kanamycin was added to the bacterial cultures with a final concentration of 200 μg ml^{-1} when necessary. The cultivation temperature of *Geobacter* and *E. coli* strains was 30 and 37°C, respectively. The bacterial growth curves were obtained by measuring the absorbance of cultures at 600 nm (OD$_{600}$). Table 1 lists all the bacterial strains used in this study.

DNA manipulation and reagents

Genomic DNA of *G. sulfurreducens* was isolated using the MiniBEST Bacteria Genomic DNA Extraction Kit

TABLE 1 Bacterial strains and plasmids used in this study

Strains or plasmids	Relevant genotype or uses	Source or reference
Bacterial strains		
G. sulferreducens		
PCA	Wild-type *G. sulferreducens*	Liu et al. (2015)
Control strain	*G. sulferreducens* PCA containing empty pAWP78 vector	This study
GNW1	*G. sulferreducens* PCA containing pOEpilA	This study
GNW2	*G. sulferreducens* PCA containing pOEomcZ	This study
GNW3	*G. sulferreducens* PCA containing pOEomcS	This study
GNW4	*G. sulferreducens* PCA containing pOEomcT	This study
E. coli DH5α	Host for vector cloning	Takara Co. Inc., Japan
Plasmids		
pAWP78	IncP-based broad host range vector	Puri et al. (2015)
pOEpilA	Expression cassette of *pilA* in pAWP78	This study
pOEomcZ	Expression cassette of *omcZ* in pAWP78	This study
pOEomcS	Expression cassette of *omcS* in pAWP78	This study
pOEomcT	Expression cassette of *omcT* in pAWP78	This study

(TaKaRa) as the template for PCR cloning of *pilA*, *omcZ*, *omcS* and *omcT* (Table S1). The start codon of *pilA* gene was changed from TTG (Richter et al., 2012) into ATG via site-directed mutagenesis by PCR. As *omcT* and *omcS* share the same promoter (Mahadevan et al., 2008; Mehta et al., 2005), the promoter and *omcT* coding region were amplified individually and then ligated. The plasmids were prepared with the QIAprep Spin Miniprep Kit (Qiagen). PCR amplification of the backbone of pAWP78 vector (Addgene No. 61263) was performed as described previously (Puri et al., 2015). All the PCR reactions were performed using the PrimeSTAR HS (Premix) Kit (TaKaRa, Japan) with high-fidelity DNA polymerase. The PCR products were purified using the GeneJET Gel Extraction Kit (Thermo Fisher Scientific).

Gene fragments and pAWP78 vector were ligated to produce the following expression constructs, pOEpilA, pOEomcZ, pOEomcS and pOEomcT. Ligation was performed using Gibson Assembly Cloning Kit (NEB) based on the overlapping sequences added at the 5′-end of primers (Table S1). The ligation products were transformed into *E. coli* DH5α, and bacterial cells were incubated on LB plates with kanamycin. Positive clones were screened by colony PCR followed by bidirectional sequencing. Sequencing-confirmed constructs were electroporated into *G. sulfurreducens* PCA (Coppi et al., 2001). Empty pAWP78 vector was transformed into *G. sulfurreducens* PCA as a control. The sequences of all the expression cassettes are shown in the supplementary materials (Table S2).

If not mentioned, analytical grade or biochemistry grade chemicals were purchased from the Sinopharm Chemical Reagent Co. Ltd or Sigma-Aldrich Co. Llc.

Western blot analysis

Polyclonal antibodies specific for PilA, OmcZ, OmcS and OmcT were prepared by Proteintech Group, Inc (Wuhan, China). Equal amounts of cells were lysed by protein-loading butter for the constructed strains and the control. Ten microliters of cell lysates were used to perform sodium dodecyl sulphate–polyacrylamide gel electrophoresis (SDS-PAGE). Following SDS-PAGE, the proteins were probed and visualized by Western blot with the antibodies of each nanowire protein, goat anti-rabbit IgG-HRP (TransGen Biotech) and super sensitive ECL luminescence reagent (Meilunbio).

Fe(III) reductions

All constructed strains were tested for their ability to reduce ferric citrate or ferrihydrite as described before (Liu et al., 2015). Ferrihydrite was synthesized and characterized as previously described (Liu et al., 2015). At predetermined time points, the produced Fe(II) was determined with the ferrozine assay (Stookey, 1970).

Biofilm assays

Geobacter sulfurreducens strains with OD_{600} of 0.1 were grown at 30°C with fumarate in 24-well plates for biofilm assay (Hu et al., 2019). At predetermined time points, the plates were washed twice using phosphate buffer solution (PBS, pH = 7.0). The bacterial biofilms on plates were stained with 0.1% crystal violet solution for 15 min. After washing twice with PBS, the stained

biofilm was dissolved and suspended in 1.0 ml ethanol solution (95%). OD_{570} was measured with a SpectraMax 190 microplate reader (Molecular Devices).

Construction of MFC

Dual-chamber MFCs with 140 ml working volume were used to evaluate the current-producing capacity of the bacterial strains. Anode and cathode chambers were separated by Nafion 117 membranes (DuPont Inc.) as previously described (Li et al., 2018). Carbon cloth was used as the electrodes. Dimensions of the anode and cathode were 1.0×1.0 cm (i.e. the geometric area is 1.0 cm^2) and 2.5×3.0 cm, respectively. The anodic electrolyte was prepared by replacing fumarate in NBFA medium with equal molar concentration of sodium chloride. The cathodic electrolyte contained $K_3[Fe(CN)_6]$, K_2HPO_4 and KH_2PO_4 (50 mM each). Mid-log *G. sulfurreducens* culture suspension was inoculated into 50 ml fresh medium and incubated at 30°C until OD_{600} of the culture reached 0.5. The bacterial cells were harvested by centrifugation at 5000 *g*, and the supernatant were discarded. Then, the cell pellets were re-suspended in 140 ml anodic electrolyte supplemented with kanamycin for maintaining the expression constructs. Subsequently, the cell suspension was injected into anode chamber. During growth of electroactive biofilm, the anode and cathode were connected by a 2 kΩ external resistor to measure the voltage generated. The potential of MFCs was recorded with a PS2024V multi-channel data acquisition unit (SMACQ, China). The MFCs of each *G. sulfurreducens* strain were set up in triplicates and repeated at least three times.

Electrochemical analyses

Electrochemical, biochemical and microscopical analyses of MFCs were performed upon reaching the highest output voltage of each MFC, that is 160, 190, 180, 140 and 160 h for the control strain, GNW1, GNW2, GNW3 and GNW4, respectively. Electrochemical analysis was carried out on a CHI 1000C multichannel potentiostat (CH Instruments, China) as previously described (Li et al., 2018). EIS was measured at the open circuit potential (OCP). The sinusoidal excitation signal was set as 10 mV and the frequency varied linearly from 10,000 to 0.01 Hz. To generate polarization curves, LSV analysis was performed on a two-electrode mode with a scan rate of 0.1 mV s^{-1} from OCP to –0.1 V. Power density (P) was calculated by $P = VIS^{-1}$, where V is the output voltage, I is the current, and S is the projected area of the anode surfaces. Cyclic voltammetry (CV) curves were obtained in a three-electrode system with

an Ag/AgCl reference electrode by voltage scanning at a rate of 5 mV s^{-1} from –0.7 to 0.1 V.

Biofilm imaging

Biofilms on the anodic carbon cloth were stained using the LIVE/DEAD BacLight Viability Kit (Thermo Fisher Scientific) as suggested from the manufacturer's instructions. The structure of electroactive biofilms was characterized via three-dimensional fluorescent images taken using an TCS SP8 confocal microscope (Leica). To display the biomass of live cells, only green fluorescence at 500 nm was detected in the confocal imaging. Image processing was implemented in the LAS AF Lite-version 2.3.0 software.

Measurement of the bacterial proteins on electrodes

To measure the amounts of proteins on the anodes, the anodic carbon cloths were cut into pieces and placed in 5 ml of 0.2 M NaOH solution. After vertexing for 1 min, bacterial cells were lysed by incubating the tube at 96°C for 20 min. The lysate was cooled to room temperature and total protein concentrations in the extracts were measured with the bicinchoninic acid protein assay kit (Beyotime). According to the manufacture's protocol, colour reactions were developed in 96-well plates and the absorbance of product solution was measured at 562 nm using a SpectraMax 190 microplate reader (Molecular Devices). The standard curve of absorbance against protein concentrations was created using bovine serum albumin solutions with defined concentrations.

Statistical analysis

The differences between the constructed strains and the control strain in different measurements were examined by independent-samples *t*-test with SPSS 20.0 for Windows, and differences were considered to be significant at $p < 0.05$.

RESULTS AND DISCUSSION

Growths and Fe(III) reductions

In this study, we constructed four *G. sulfurreducens* strains with the expression vectors of nanowire proteins, namely, GNW1 (pOEpilA), GNW2 (pOEomcZ), GNW3 (pOEomcS) and GNW4 (pOEomcT) (Table 1). Western blot analyses confirmed that PilA, OmcZ, OmcS and

OmcT proteins were overexpressed in GNW1, GNW2, GNW3 and GNW4, respectively (Figure S1). All the constructed strains grew slower than the control strain (i.e. *G. sulfurreducens* PCA with empty pAWP78 vector) with fumarate as the electron acceptor (Figure S2). This finding suggested that overexpression of the nanowires maybe a metabolic burden and thus decreased cell growth. However, the constructed strains reduced soluble ferric citrate at comparable rates (Figure 1A). It was also shown that ferrihydrite reduction by GNW1 and GNW3 was slightly faster than the remaining constructed and control strains (Figure 1B). These results are consistent with previous reports that nanowires were not needed for reducing soluble Fe(III) and that PilA and OmcS have critical roles in reducing solid-phase Fe(III) (Liu et al., 2014, 2018; Mehta et al., 2005; Nevin et al., 2009; Reguera et al., 2005).

Biofilm formation

After inoculation in the 24-well plates, all the *G. sulfurreducens* strains formed cohesive biofilms on the bottom of the plate wells. The biomass of the biofilms reached their peaks between the 4th and 5th day and decreased subsequently (Figure 2). Compared with the control strain, biomass of the biofilms from the constructed strains increased 16% to 146% ($p < 0.05$), which decreased in the order of GNW2 > GNW1 > GNW3 > GNW4 > control strain. To evaluate the effects of nanowire proteins on the biofilm-forming capability of individual cells, the ratios of biofilm biomass to cell growth at the 4th day were calculated (Figure S3). The ratios for the

constructed strains were significantly higher than that for the control strain ($p < 0.05$). These results revealed that overexpression of PilA, OmcZ, OmcS and OmcT can promote the formation of *G. sulfurreducens* biofilm. Previous study also found that PilA deficiency impaired the biofilm formation of *G. sulfurreducens* on solid surface when fumarate was used as electron acceptor (Reguera et al., 2007; Richter et al., 2012). These findings suggested that pili plays an important structural role in cell–cell aggregation during biofilm differentiation (Reguera et al., 2007, Richter et al., 2012). On the other hand, *Geobacter* pili may mediate the secretion of OmcS and OmcZ (Gu et al., 2021). In addition to their electron transfer roles, cytochromes may act as important structural components in biofilm matrix (Hu et al., 2021). Similarly, the results of this investigation also indicated the structural roles of OmcZ, OmcS and OmcT in biofilm formation. Comparison between the constructed strains also revealed that overexpression of OmcZ had the most significant promotion for biofilm formation in well plate, which provided further evidence for an important role of OmcZ in maintaining biofilm structure.

Bioelectrochemical characterizations

During the incubation period in the MFCs, the peak voltage outputs of the constructed *G. sulfurreducens* strains were 0.470–0.578V in comparison with a peak value of 0.355V for the control strain ($p < 0.05$) (Figure S4). The maximum values of electrochemical curves were used for the following analyses. As shown
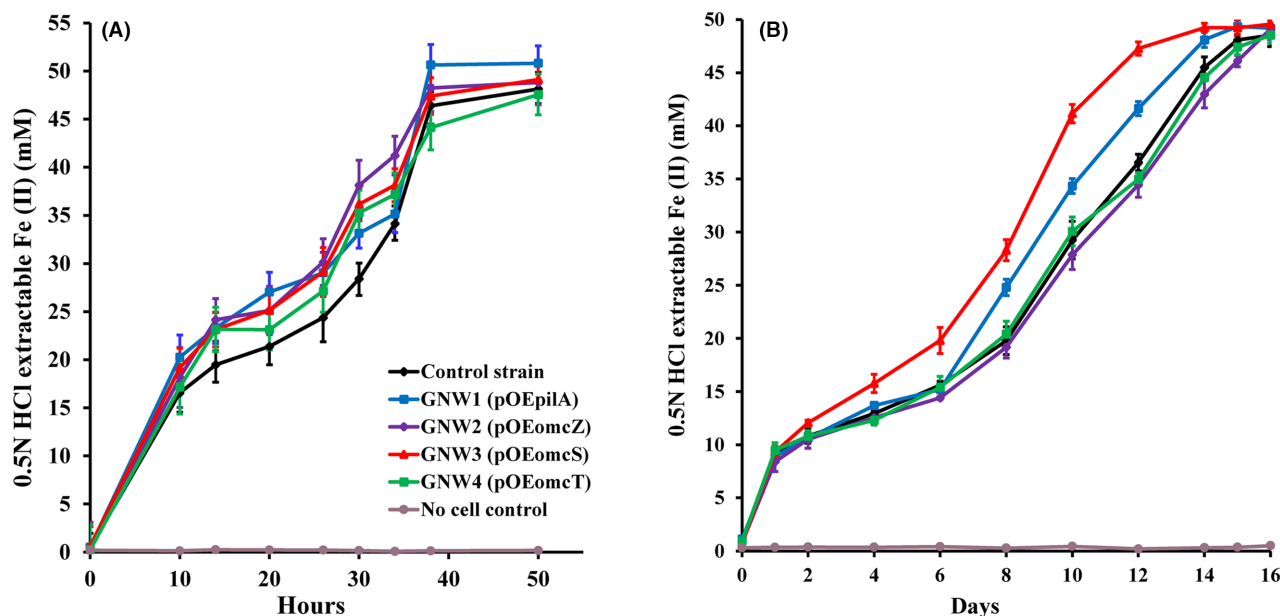
FIGURE 1 Reduction in ferric citrate (A) and ferrihydrite (B) by the control and the constructed *G. sulfurreducens* strains. The expression constructs are displayed in parentheses. The values reported are the means and standard deviations of triplicate measurements.

FIGURE 2 Biofilm formation of the control and the constructed *G. sulfurreducens* strains. OD_{570}, optical density at 570 nm. The expression constructs are displayed in parentheses. The values reported are the means and standard deviations of triplicate measurements. Asterisks represent significant differences between the constructed *G. sulfurreducens* strains and the control strain at the same day ($p < 0.05$).
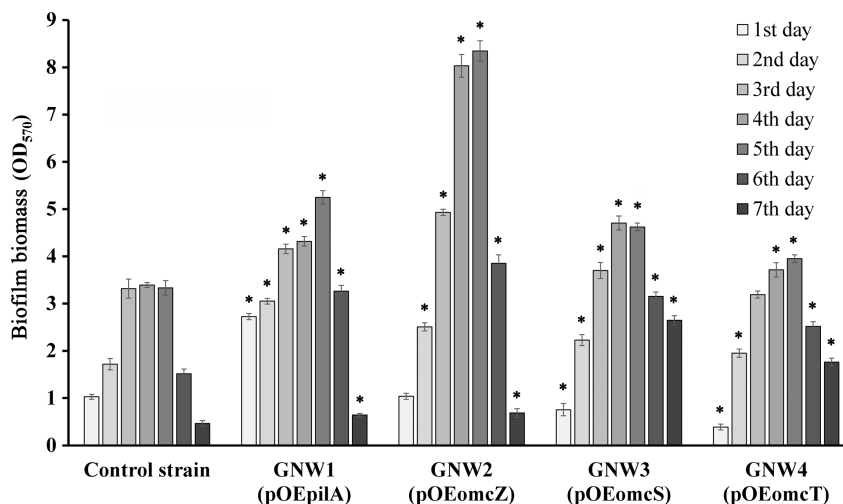
in Figure 3A, the calculated current output of GNW3 and GNW4 increased much faster than the control strain, indicating that overexpression of OmcS and OmcT enhanced the attachment of *G. sulfurreducens* to electrode. Compared with the control strain, all the constructed strains generated much higher electrical outputs that increased by 32% to 62% ($p < 0.05$) (Figure 3A). The maximum current density of the constructed strains was 2.35 ± 0.06 Am^{-2} ($n = 3$) to 2.89 ± 0.06 Am^{-2} ($n = 3$), while the control strain only produced 1.78 ± 0.05 Am^{-2} ($n = 3$) (Figure 3A).

The polarization curves of the constructed strains were very similar and increased much faster than that of the control strain under linear sweep voltammetry (LSV) conditions (Figure 3B). As shown on the power output curves (Figure 3C), the power density of the constructed strains was elevated by 2.62- to 2.97-fold in comparison with that of the control strain ($p < 0.05$). The constructed strains produced the maximum power density of 1.39 ± 0.08 Wm^{-2} ($n = 3$) to 1.58 ± 0.08 Wm^{-2} ($n = 3$), while the control strain only produced 0.53 ± 0.62 Wm^{-2} ($n = 3$). Considering that the polarization curves reflect the increase of current density with the reduction in external potential, the reducing slope of polarization curves is thus positively correlated with the internal resistance of the MFCs. Compared with the control MFC, the MFCs of the constructed strains had very small reducing slope at the linear portion of the polarization curves (Figure 3B), and therefore their internal resistance was smaller. This finding was also evidenced by the data of electrochemical impedance spectroscopy (EIS) (Figure 3D). The diameter of the semicircle appearing in the Nyquist plots is positively correlated with charge transfer resistance (Malvankar et al., 2012). The MFCs of the constructed strains had shorter diameters in the Nyquist plots than that of the control strain ($p < 0.05$) (Figure 3D), indicating that overexpressed nanowires effectively reduced the charge transfer resistance of MFCs. Similarly, previous electrochemical impedance analysis revealed that the

biofilm of an OmcZ-deficient mutant was more electrically resistant than that of the wild-type *G. sulfurreducens* (Richter et al., 2009).

Results in this study demonstrate for the first time that overexpression of nanowire proteins can enhance current production through decreasing the internal resistance of MFCs. These findings are also consistent with the fact that the conductivity of protein nanowires is the critical factor for current production of electrode-attached biofilms (Liu et al., 2021; Lovley & Walker, 2019; Wang et al., 2019; Yalcin et al., 2020). However, given that the known nanowire proteins have distinct electrochemical properties (Gu et al., 2021; Wang et al., 2019; Yalcin et al., 2020; Yalcin & Malvankar, 2020), the similar power density of the constructed strains is unexpected. According to the shape of polarization curves, the electrical output efficiency of MFCs probably reached the limitation of substrate turnover rate, which might be caused by the limited metabolic rate of *G. sulfurreducens*, or the substrate diffusion limitation between biofilm and bulk solution.

The kinetics of redox reactions at cell-electrode interfaces were also determined by cyclic voltammetry (CV) analysis through measuring current response at a low scan rate of voltage (Figure 4). The current density at the redox peaks of all the constructed strains showed significant increase compared with that of the control strain, indicating improved electroactivity of biofilms derived from the constructed strains. Previous investigation demonstrated that the peak current of CV curves is positively correlated with the cell density at the electrode surface and the number of membrane-bound electron transfer proteins in the individual cells (Fricke et al., 2008). Therefore, the results of CV analysis were consistent with the increased biomass of electrode-attached biofilms observed in the following section and overexpression of nanowire proteins in *G. sulfurreducens*.

The first derivatives of CV data were used to calculate the midpoint potentials of electrode-attached
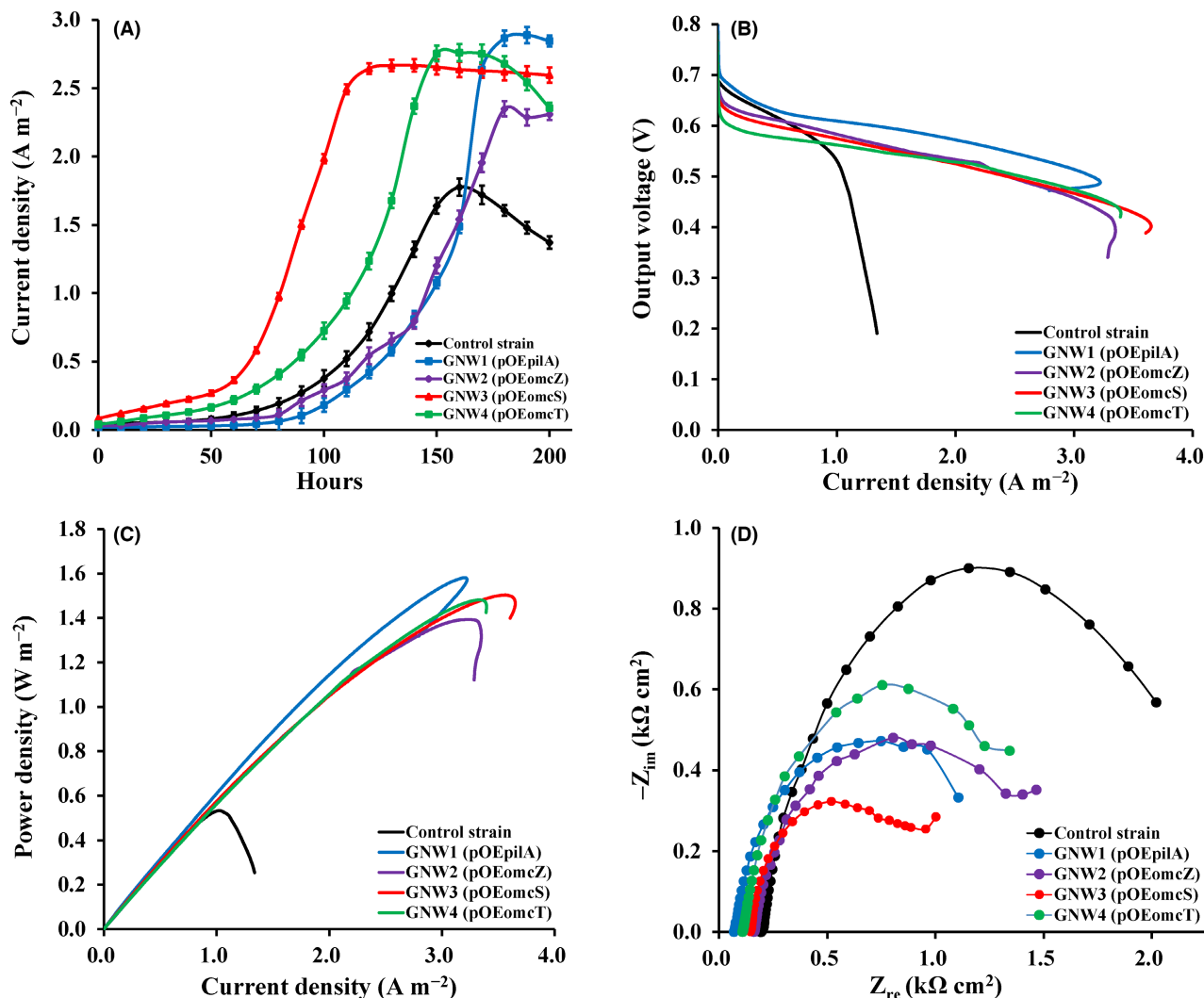
FIGURE 3 Bioelectrochemical characterization of the control and the constructed *G. sulfurreducens* strains. (A) Current output curves, the values reported are the means and standard deviations of triplicate measurements; (B) polarization curves (output voltage vs. current density) generated by LSV at the scan rate of $0.1\,mV\,s^{-1}$; (C) power density output curves (power density vs. current density); (D) Nyquist plots of MFCs. The expression constructs are displayed in parentheses. Curves in (B), (C) and (D) are representative ($n = 3$).

biofilms (Figure S5). GNW3 and the control strain had the same midpoint potential of $-0.39\,V$ (vs. Ag/AgCl). The midpoint potential of GNW1, GNW2 and GNW4 is between $-0.37\,V$ (vs. Ag/AgCl) and $-0.36\,V$ (vs. Ag/AgCl), higher than that of the control strain. Given that the midpoint potentials of OmcZ and OmcS are $-0.42\,V$ (vs. Ag/AgCl) and $-0.41\,V$ (vs. Ag/AgCl) respectively (Fricke et al., 2008; Inoue et al., 2010; Qian et al., 2011), GNW2 and GNW3 were expected to have midpoint potentials lower than that of the control strain, which was inconsistent with the present results. Therefore, these findings indicated a complex regulation of redox components in *G. sulfurreducens* as suggested in previous studies (Hernández-Eligio et al., 2022; Park & Kim, 2011). In addition, reversible peaks near the top of the CV curves at approximately $-0.30\,V$ (vs. Ag/AgCl) were resolved in all the biofilms of the constructed strains. First derivate analysis also revealed a current

wave near $-0.30\,V$ (vs. Ag/AgCl) for the control strain (Figure S5). Therefore, this reversible peak reflects an intrinsic electrochemical characteristic of *G. sulfurreducens* biofilm.

Biomass and images of electrode-attached biofilms

The protein amounts of the electrode-attached biofilms were measured to evaluate the abundance of electroactive cells on the anode (Figure 5). The protein amounts of the constructed strains increased by 39% to 62%, as compared with that of the control strain ($p < 0.05$). The amounts of proteins from the biofilms of the constructed strains ranged from $7.23 \pm 0.36\,g\,m^{-2}$ ($n = 3$) to $8.45 \pm 0.35\,g\,m^{-2}$ ($n = 3$), while those for the biofilms of the control strain was $5.21 \pm 0.28\,g\,m^{-2}$ ($n = 3$).
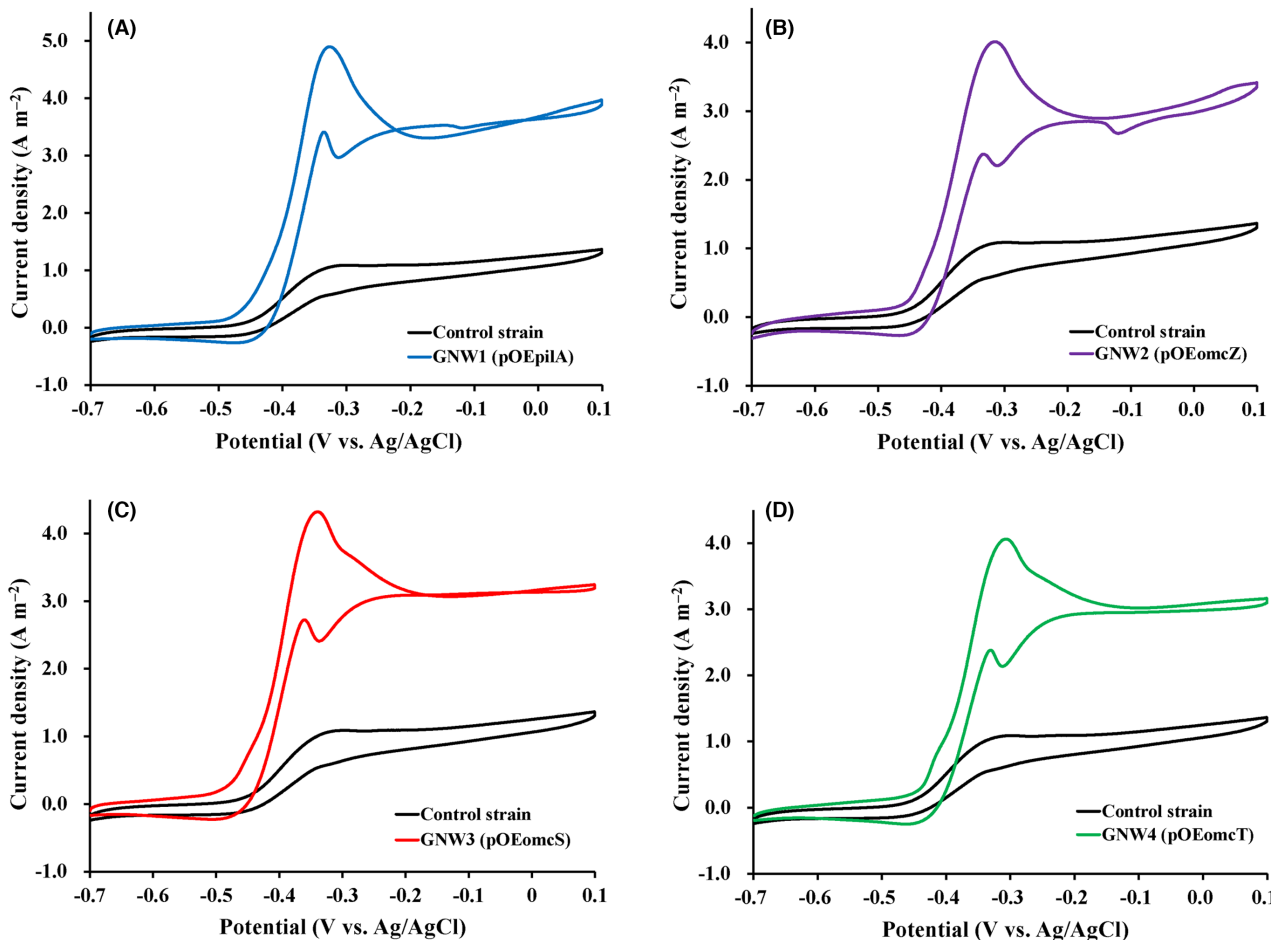
FIGURE 4 CV curves obtained at the scan rate of 5 mV s^{-1}. Shown are the CV data of the control strain and the constructed *G. sulfurreducens* strains overexpressing PilA (A), OmcZ (B), OmcS (C) and OmcT (D). The expression constructs are displayed in parentheses. Curves are representative ($n = 3$).

FIGURE 5 Protein amounts of electrode-attached biofilms and biofilm biomass-normalized maximum power density. Shown are the amounts of proteins normalized with the areas of anodes. The maximum power density was normalized with the biofilm-associated protein amounts. The values reported are the means and standard deviations of triplicate measurements. The expression constructs are displayed in parentheses. Asterisks represent significant differences between the constructed *G. sulfurreducens* strains and the control strain ($p < 0.05$).
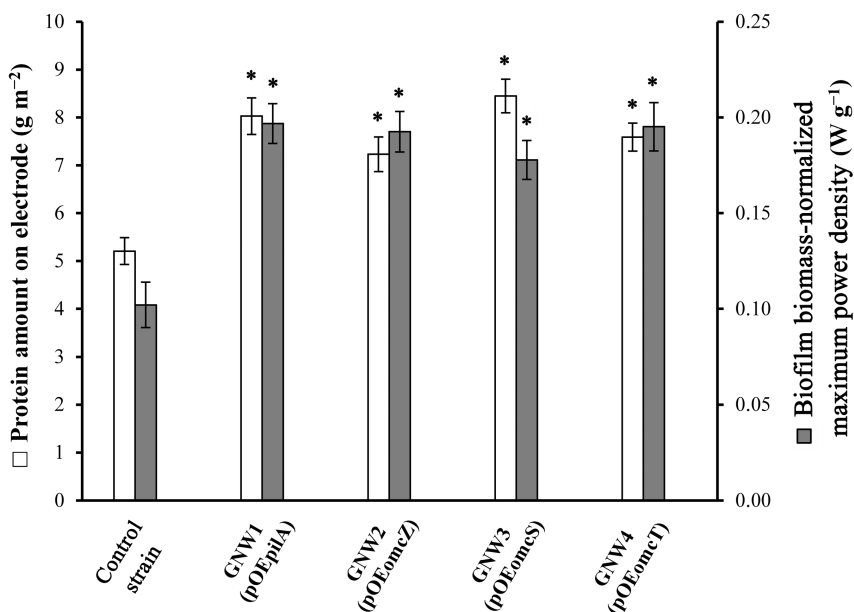
In addition, comparison between the constructed strains revealed that overexpression of OmcS had the most significant enhancement for biofilm formation on electrode. However, overexpression of OmcZ had relatively weaker promotion for electroactive biofilm. This result may be ascribed to the inhibition of *omcZ* gene

(A)

(B)

(C)

(D)

(E)
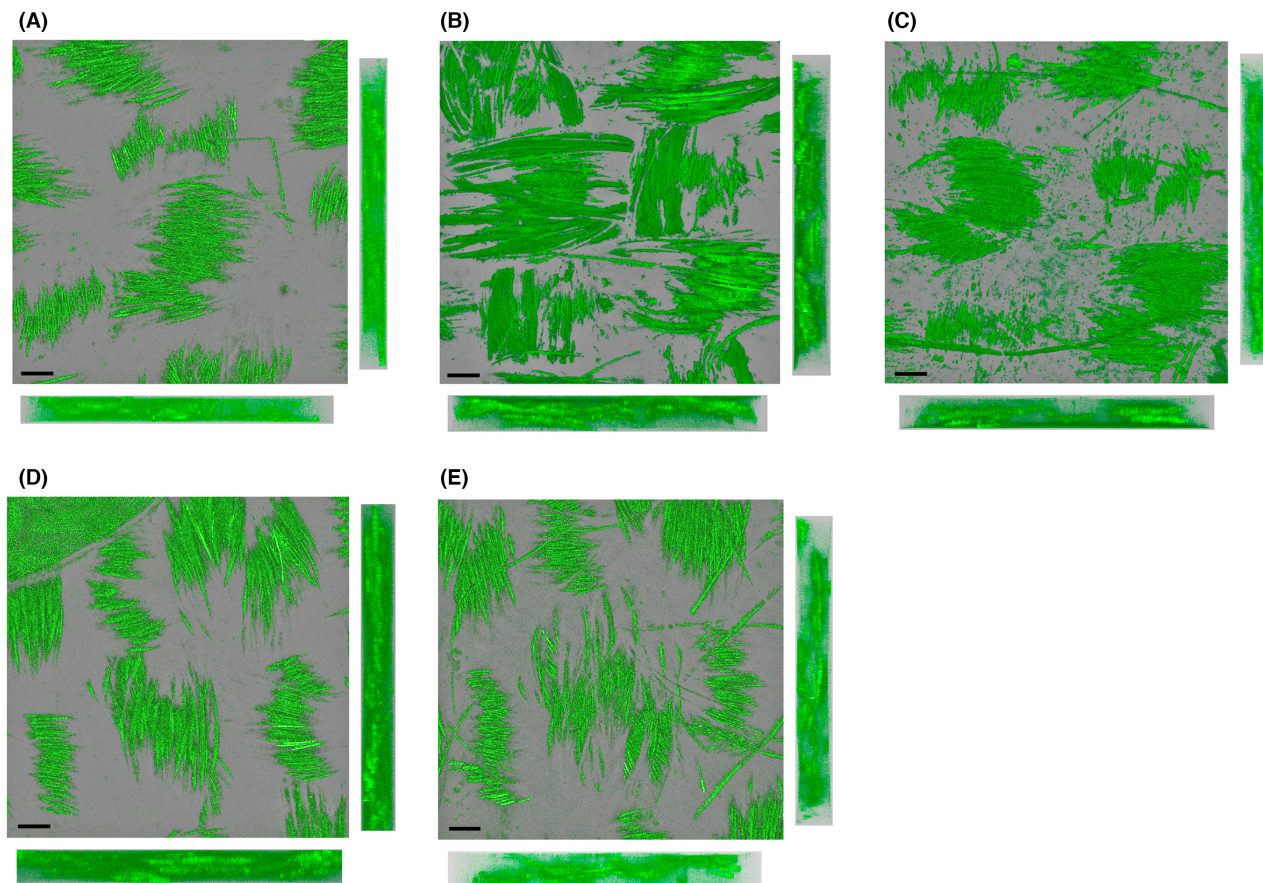
FIGURE 6 Confocal scanning laser microscopy images of the electrode-attached *G. sulfurreducens* biofilms. (A) control strain; (B) GNW1 (pOEpilA); (C) GNW2 (pOEomcZ); (D) GNW3 (pOEomcS); (E) GNW4 (pOEomcT). The images are three-dimensional top views (middle panels), lateral side views (right panels) and horizontal side views (bottom panels) of biofilms. Side-view images show denser biofilms for the constructed strains with overexpression of nanowire proteins than that for the control strain. Images are representative (n = 5). Scale bar, 100 μm.

on the expression of *omcS* gene (Park & Kim, 2011). After normalization with measured proteins, the maximum power density of the constructed strains was $0.18 \pm 0.01 \, W \, g^{-1}$ (n = 3) to $0.20 \pm 0.01 \, W \, g^{-1}$ (n = 3), which were 1.74- to 1.93-fold higher than that of the control strain with $0.10 \pm 0.01 \, W \, g^{-1}$ (n = 3) ($p < 0.05$) (Figure 5).

As shown in Figure 6, *Geobacter* cells formed active biofilms on the surface of the carbon filaments of anodes. Three-dimensional side-view image revealed that the thickness of biofilms from the constructed strains was 110–130 μm, which were significantly larger than the thickness of biofilms from the control strain with only 75 ± 13 μm (n = 3) ($p < 0.05$). These results further evidenced the measured larger protein amounts of the constructed strains.

Enhancement of biofilm-formation capability was thought to be beneficial for increasing the abundance of active current-producing cells on electrode. In this study, the biomass of electrode-attached biofilm was increased for all constructed strains, and the current production was substantially improved. Moreover, increase in average power output normalized with protein

amounts suggested that the EET efficiency of individual cells was also improved. These results were consistent with previous reports that PilA and OmcZ were critical components of conductive biofilms (Inoue et al., 2011; Nevin et al., 2009; Steidl et al., 2016). In previous study, the abundance of OmcS was positively correlated with the current productivity of electrode-attached biofilm (Holmes et al., 2006). Consistent with this finding, the results from this study showed that overexpressed OmcS and OmcT also participated in electron transfer to electrodes. In addition, the present results revealed that the constructed strain with overexpressed OmcZ had lower current production than that with overexpressed OmcS. Given that *omcZ* can downregulate *omcS* expression (Park & Kim, 2011), the total abundance of extracellular cytochromes of the biofilms with overexpression of *omcZ* may be lower than that with overexpression of *omcS*. Thus, the results from this investigation suggested that all the *Geobacter* nanowire components play important roles in the development of conductive biofilm.

Up to date, several genetic strategies have been developed to engineer *G. sulfurreducens* for improving

its EET efficiency and current production (Dantas et al., 2015; Hernández-Eligio et al., 2022; Leang et al., 2013; Tan et al., 2017). All these studies indicated the importance of protein nanowires for the formation of thick conductive biofilms as emphasized in this study. Therefore, bacterial nanowire proteins are promising synthetic biology parts for improving electrochemical performance of microbes by genetic engineering. Moreover, protein nanowires are interesting conductive bionanomaterials which can be constructed in *G. sulfurreducens* at low cost (Liu et al., 2020).

CONCLUSIONS

Overexpression of nanowire proteins (e.g. PilA, OmcZ, OmcS and OmcT) can substantially increase electrical outputs of the MFCs with *G. sulfurreducens*. The increased bioelectricity production was attributed to the decreased internal resistance as well as improved biofilm formation on the anodes. These results demonstrate a new approach for enhancing the performance of MFCs. It should be noted that overexpression of nanowire proteins may cause metabolic burden for constructed cells and the performance of MFCs is close to the upper limit in this study. Rational engineering of the metabolic flux of *G. sulfurreducens* may further improve the electricity production of MFCs with this species.

CONFLICT OF INTEREST
The authors declare no competing interests.

DATA AVAILABILITY STATEMENT
The data that support the findings of this study are available from the corresponding author.

ORCID
Yongguang Jiang ![ORCID] https://orcid.org/0000-0002-3829-7423

REFERENCES
Coppi, M.V., Leang, C., Sandler, S.J. & Lovley, D.R. (2001) Development of a genetic system for *Geobacter sulfurreducens*. *Applied and Environmental Microbiology*, 67, 3180–3187.

Dantas, J.M., Morgado, L., Aklujkar, M., Bruix, M., Londer, Y.Y., Schiffer, M. et al. (2015) Rational engineering of *Geobacter sulfurreducens* electron transfer components: a foundation for building improved *Geobacter*-based bioelectrochemical technologies. *Frontiers in Microbiology*, 6, 752.

Fricke, K., Harnisch, F. & Schröder, U. (2008) On the use of cyclic voltammetry for the study of anodic electron transfer in microbial fuel cells. *Energy & Environmental Science*, 1, 144–147.

Gu, Y., Srikanth, V., Salazar-Morales, A.I., Jain, R., O'Brien, J.P., Yi, S.M. et al. (2021) Structure of *Geobacter* pili reveals secretory rather than nanowire behaviour. *Nature*, 597, 430–434.

Hernández-Eligio, A., Huerta-Miranda, G.A., Martínez-Bahena, S., Castrejón-López, D., Miranda-Hernández, M. & Juárez, K. (2022) GSU1771 regulates extracellular electron transfer and electroactive biofilm formation in *Geobacter sulfurreducens*: genetic and electrochemical characterization. *Bioelectrochemistry*, 145, 108101.

Holmes, D.E., Chaudhuri, S.K., Nevin, K.P., Mehta, T., Methé, B.A., Liu, A. et al. (2006) Microarray and genetic analysis of electron transfer to electrodes in *Geobacter sulfurreducens*. *Environmental Microbiology*, 8, 1805–1815.

Hu, Y., Liu, X., Ren, A.T.M., Gu, J.D. & Cao, B. (2019) Optogenetic modulation of a catalytic biofilm for the biotransformation of indole into tryptophan. *ChemSusChem*, 12, 5142–5148.

Hu, Y., Wang, Y., Han, X., Shan, Y., Li, F. & Shi, L. (2021) Biofilm biology and engineering of *Geobacter* and *Shewanella* spp. for energy applications. *Frontiers in Bioengineering and Biotechnology*, 9, 786416.

Inoue, K., Qian, X., Morgado, L., Kim, B.C., Mester, T., Izallalen, M. et al. (2010) Purification and characterization of OmcZ, an outer-surface, octaheme c-type cytochrome essential for optimal current production by *Geobacter sulfurreducens*. *Applied and Environmental Microbiology*, 76, 3999–4007.

Inoue, K., Leang, C., Franks, A.E., Woodard, T.L., Nevin, K.P. & Lovley, D.R. (2011) Specific localization of the c-type cytochrome OmcZ at the anode surface in current-producing biofilms of *Geobacter sulfurreducens*. *Environmental Microbiology Reports*, 3, 211–217.

Jiang, Y., Shi, M. & Shi, L. (2019) Molecular underpinnings for microbial extracellular electron transfer during biogeochemical cycling of earth elements. *Science China. Life Sciences*, 62, 1275–1286.

Jiménez Otero, F., Chadwick, G.L., Yates, M.D., Mickol, R.L., Saunders, S.H., Glaven, S.M. et al. (2021) Evidence of a streamlined extracellular electron transfer pathway from biofilm structure, metabolic stratification, and long-range electron transfer parameters. *Applied and Environmental Microbiology*, 87, e0070621.

Leang, C., Malvankar, N.S., Franks, A.E., Nevin, K.P. & Lovley, D.R. (2013) Engineering *Geobacter sulfurreducens* to produce a highly cohesive conductive matrix with enhanced capacity for current production. *Energy and Environmental Science*, 6, 1901–1908.

Li, F., Li, Y., Cao, Y., Wang, L., Liu, C., Shi, L. et al. (2018) Modular engineering to increase intracellular NAD(H/+) promotes rate of extracellular electron transfer of *Shewanella oneidensis*. *Nature Communications*, 9, 3637.

Liu, X., Tremblay, P.-L., Malvankar, N.S., Nevin, K.P., Lovley, D.R. & Vargas, M. (2014) A *Geobacter sulfurreducens* strain expressing *Pseudomonas aeruginosa* type IV pili localizes OmcS on pili but is deficient in Fe(III) oxide reduction and current production. *Applied and Environmental Microbiology*, 80, 1219–1224.

Liu, Y., Fredrickson, J.K., Zachara, J.M. & Shi, L. (2015) Direct involvement of *ombB*, *omaB*, and *omcB* genes in extracellular reduction of Fe(III) by *Geobacter sulfurreducens* PCA. *Frontiers in Microbiology*, 6, 1075.

Liu, X., Zhuo, S., Rensing, C. & Zhou, S. (2018) Syntrophic growth with direct interspecies electron transfer between pili-free *Geobacter* species. *The ISME Journal*, 12, 2142–2151.

Liu, X., Gao, H., Ward, J.E., Liu, X., Yin, B., Fu, T. et al. (2020) Power generation from ambient humidity using protein nanowires. *Nature*, 578, 550–554.

Liu, X., Walker, D.J.F., Nonnenmann, S.S., Sun, D. & Lovley, D.R. (2021) Direct observation of electrically conductive pili emanating from *Geobacter sulfurreducens*. *MBio*, 12, e0220921.

Logan, B.E., Rossi, R., Ragab, A.A. & Saikaly, P.E. (2019) Electroactive microorganisms in bioelectrochemical systems. *Nature Reviews. Microbiology*, 17, 307–319.

Lovley, D.R. & Walker, D.J.F. (2019) *Geobacter* protein nanowires. *Frontiers in Microbiology*, 10, 2078.

Mahadevan, R., Yan, B., Postier, B., Nevin, K.P., Woodard, T.L., O'Neil, R. et al. (2008) Characterizing regulation of metabolism in *Geobacter sulfurreducens* through genome-wide expression data and sequence analysis. *OMICS*, 12, 33–59.

Malvankar, N.S., Tuominen, M.T. & Lovley, D.R. (2012) Biofilm conductivity is a decisive variable for high-current-density *Geobacter sulfurreducens* microbial fuel cells. *Energy and Environmental Science*, 5, 5790–5797.

Mateo, S., Cañizares, P., Fernandez-Morales, F.J. & Rodrigo, M.A. (2018) A critical view of microbial fuel cells: what is the next stage? *ChemSusChem*, 11, 4183–4192.

Mehta, T., Coppi, M.V., Childers, S.E. & Lovley, D.R. (2005) Outer membrane c-type cytochromes required for Fe(III) and Mn(IV) oxide reduction in *Geobacter sulfurreducens*. *Applied and Environmental Microbiology*, 71, 8634–8641.

Nevin, K.P., Richter, H., Covalla, S.F., Johnson, J.P., Woodard, T.L., Orloff, A.L. et al. (2008) Power output and columbic efficiencies from biofilms of *Geobacter sulfurreducens* comparable to mixed community microbial fuel cells. *Environmental Microbiology*, 10, 2505–2514.

Nevin, K.P., Kim, B.-C., Glaven, R.H., Johnson, J.P., Woodard, T.L., Methé, B.A. et al. (2009) Anode biofilm transcriptomics reveals outer surface components essential for high density current production in *Geobacter sulfurreducens* fuel cells. *PLoS One*, 4, e5628.

Park, I. & Kim, B.-C. (2011) Homologous overexpression of *omcZ*, a gene for an outer surface c-type cytochrome of *Geobacter sulfurreducens* by single-step gene replacement. *Biotechnology Letters*, 33, 2043–2048.

Puri, A.W., Owen, S., Chu, F., Chavkin, T., Beck, D.A.C., Kalyuzhnaya, M.G. et al. (2015) Genetic tools for the industrially promising methanotroph *Methylomicrobium buryatense*. *Applied and Environmental Microbiology*, 81, 1775–1781.

Qian, X.L., Mester, T., Morgado, L., Arakawa, T., Sharma, M.L., Inoue, K. et al. (2011) Biochemical characterization of purified OmcS, a c-type cytochrome required for insoluble Fe(III) reduction in *Geobacter sulfurreducens*. *Biochimica et Biophysica Acta - Bioenergetics*, 1807, 404–412.

Reguera, G. & Kashefi, K. (2019) The electrifying physiology of *Geobacter* bacteria, 30 years on. *Advances in Microbial Physiology*, 74, 1–96.

Reguera, G., McCarthy, K.D., Mehta, T., Nicoll, J.S., Tuominen, M.T. & Lovley, D.R. (2005) Extracellular electron transfer via microbial nanowires. *Nature*, 435, 1098–1101.

Reguera, G., Nevin, K.P., Nicoll, J.S., Covalla, S.F., Woodard, T.L. & Lovley, D.R. (2006) Biofilm and nanowire production leads to increased current in *Geobacter sulfurreducens* fuel cells. *Applied and Environmental Microbiology*, 72, 7345–7348.

Reguera, G., Pollina Rachael, B., Nicoll Julie, S. & Lovley Derek, R. (2007) Possible nonconductive role of *Geobacter sulfurreducens* pilus nanowires in biofilm formation. *Journal of Bacteriology*, 189, 2125–2127.

Richter, H., Nevin, K.P., Jia, H., Lowy, D.A., Lovley, D.R. & Tender, L.M. (2009) Cyclic voltammetry of biofilms of wild type and mutant *Geobacter sulfurreducens* on fuel cell anodes indicates possible roles of OmcB, OmcZ, type IV pili, and protons in extracellular electron transfer. *Energy and Environmental Science*, 2, 506–516.

Richter, L.V., Sandler, S.J. & Weis, R.M. (2012) Two isoforms of *Geobacter sulfurreducens* PilA have distinct roles in pilus biogenesis, cytochrome localization, extracellular electron transfer, and biofilm formation. *Journal of Bacteriology*, 194, 2551–2563.

Rotaru, A.E., Woodard, T.L., Nevin, K.P. & Lovley, D.R. (2015) Link between capacity for current production and syntrophic growth in *Geobacter* species. *Frontiers in Microbiology*, 6, 744.

Santoro, C., Arbizzani, C., Erable, B. & Ieropoulos, I. (2017) Microbial fuel cells: from fundamentals to applications. A review. *Journal of Power Sources*, 356, 225–244.

Shi, L., Dong, H., Reguera, G., Beyenal, H., Lu, A., Liu, J. et al. (2016) Extracellular electron transfer mechanisms between microorganisms and minerals. *Nature Reviews. Microbiology*, 14, 651–662.

Shi, M., Jiang, Y. & Shi, L. (2019) Electromicrobiology and biotechnological applications of the exoelectrogens *Geobacter* and *Shewanella* spp. *SCIENCE CHINA Technological Sciences*, 62, 1670–1678.

Steidl, R.J., Lampa-Pastirk, S. & Reguera, G. (2016) Mechanistic stratification in electroactive biofilms of *Geobacter sulfurreducens* mediated by pilus nanowires. *Nature Communications*, 7, 12217.

Stookey, L.L. (1970) Ferrozine-a new spectrophotometric reagent for iron. *Analytical Chemistry*, 42, 779–781.

Strycharz, S.M., Malanoski, A.P., Snider, R.M., Yi, H., Lovley, D.R. & Tender, L.M. (2011) Application of cyclic voltammetry to investigate enhanced catalytic current generation by biofilm-modified anodes of *Geobacter sulfurreducens* strain DL1 vs. variant strain KN400. *Energy and Environmental Science*, 4, 896–913.

Tan, Y., Adhikari, R.Y., Malvankar, N.S., Ward, J.E., Woodard, T.L., Nevin, K.P. et al. (2017) Expressing the *Geobacter metallireducens* PilA in *Geobacter sulfurreducens* yields pili with exceptional conductivity. *MBio*, 8, e02203–e02216.

Vargas, M., Malvankar, N.S., Tremblay, P.-L., Leang, C., Smith, J.A., Patel, P. et al. (2013) Aromatic amino acids required for pili conductivity and long-range extracellular electron transport in *Geobacter sulfurreducens*. *MBio*, 4, e00105–e00113.

Verma, J., Kumar, D., Singh, N., Katti, S.S. & Shah, Y.T. (2021) Electricigens and microbial fuel cells for bioremediation and bioenergy production: a review. *Environmental Chemistry Letters*, 19, 2091–2126.

Wang, F., Gu, Y., O'Brien, J.P., Yi, S.M., Yalcin, S.E., Srikanth, V. et al. (2019) Structure of microbial nanowires reveals stacked hemes that transport electrons over micrometers. *Cell*, 177, 361–369.

Yalcin, S.E. & Malvankar, N.S. (2020) The blind men and the filament: understanding structures and functions of microbial nanowires. *Current Opinion in Chemical Biology*, 59, 193–201.

Yalcin, S.E., O'Brien, J.P., Gu, Y., Reiss, K., Sophia, M.Y., Jain, R. et al. (2020) Electric field stimulates production of highly conductive microbial OmcZ nanowires. *Nature Chemical Biology*, 16, 1136–1142.

Yi, H., Nevin, K.P., Kim, B.-C., Franks, A.E., Klimes, A., Tender, L.M. et al. (2009) Selection of a variant of *Geobacter sulfurreducens* with enhanced capacity for current production in microbial fuel cells. *Biosensors & Bioelectronics*, 24, 3498–3503.

Zhao, J., Li, F., Cao, Y., Zhang, X., Chen, T., Song, H. et al. (2020) Microbial extracellular electron transfer and strategies for engineering electroactive microorganisms. *Biotechnology Advances*, 53, 107682.

SUPPORTING INFORMATION

Additional supporting information can be found online in the Supporting Information section at the end of this article.